

Supporting Information

Four uncommon nanocage-based Ln-MOFs: highly selective luminescent sensing for Cu²⁺ ion and selective CO₂ capture

Bo Liu,[‡] Wei-Ping Wu,[‡] Lei Hou* and Yao-Yu Wang

Key Laboratory of Synthetic and Natural Functional Molecule Chemistry of the Ministry of Education, Shaanxi Key Laboratory of Physico-Inorganic Chemistry, College of Chemistry & Materials Science, Northwest University, Xi'an 710069, China.

Email: lhou2009@nwu.edu.cn

Materials and Measurements. All reagents and solvents were commercially available and were used without further purification. Infrared spectra were obtained in KBr discs on a Nicolet Avatar 360 FTIR spectrometer in the 400-4000 cm⁻¹ region. Photoluminescence analyses were performed on an Edinburgh FLS55 luminescence spectrometer. Elemental analyses (C, H and N) were performed with a Perkin Elmer 2400C Elemental Analyzer. Thermalgravimetric analyses (TGA) were carried out in nitrogen stream using a Netzsch TG209F3 equipment at a heating rate of 5°C/min. Powder X-ray diffraction (PXRD) data were recorded on a Bruker D8 ADVANCE X-ray powder diffractometer (Cu K α , 1.5418 Å). All the gas sorption isotherms were measured by using a ASAP 2020M adsorption equipment.

Photoluminescence Measurements. The photoluminescence and decay lifetime of **1-Eu** and **1-Tb** were investigated in the solid state at room temperature. For the experiments of sensing metal ions, **1-Eu** powder (5 mg) was immersed in DMF solutions containing 10⁻² M of M(NO₃)_x (M = Na⁺, K⁺, Mg²⁺, Ca²⁺, Zn²⁺, Cd²⁺, Mn²⁺, Co²⁺, Cu²⁺, Ni²⁺, In³⁺, or Tb³⁺) as well as the same way used for the sensing in mixed metal ions (the concentration of 10⁻² M for Cu²⁺ ion and 10⁻¹ M for other metal ions). Before photoluminescence measurements, the suspensions were oscillated for 30 min using ultrasonic waves to ensure uniform dispersion. For the titration experiments of Cu²⁺ ion, **1-Eu** powder (5 mg) was immersed in DMF or DMF solutions contain other metal ions with the dropped addition of different concentrations of Cu²⁺ in DMF.

Sorption Measurements. The activated samples were prepared by soaking the as-synthesized samples in CH₃OH for two days, then in CH₂Cl₂ for three days and subsequent heating at 120 °C in a quartz tube under high vacuum for 10 h to remove the free DMF and H₂O molecules prior to measurements.

Synthesis of [H₂N(CH₃)₂][Eu₃(L)₂(HCOO)₂(DMF)₂(H₂O)]·2DMF·20(H₂O) (1-Eu). A mixture of H₄L (12.22 mg, 0.03 mmol) and Eu(NO₃)₃·6H₂O (44.60 mg, 0.10 mmol) was dissolved in DMF (2 mL) in a screw-capped vial. After two drops of HNO₃ (63%, aq.) and 0.1 mL of H₂O were added to the mixture, the vial was capped and placed in an oven at 105 °C for 12 h. The resulting single crystals were washed with DMF three times to give **1-Eu**. The yield was ~27.1 mg (87.4% based on H₄L). Anal. Calc. for C₅₈H₉₈Eu₃N₇O₄₅: C, 33.66; H, 4.77; N, 4.74. Found: C, 33.39; H, 4.62; N, 4.81%. IR (KBr, cm⁻¹): 3402(s), 2933(m), 2492(w), 2322(w), 2026(w), 1662(m), 1435(w), 1327(m), 1279(m), 1253(m), 1179(s), 1102(s), 1062(m), 930(m), 860(m), 783(s), 719(s), 657(s), 529(m).

Synthesis of [H₂N(CH₃)₂][Ln₃(L)₂(HCOO)₂(DMF)₂(H₂O)]·2DMF·X(H₂O) (Ln = Tb, Gd and Dy; X = 20 for 1-Tb; X = 18 for 1-Gd and 1-Dy). With Tb(NO₃)₃·6H₂O (45.30 mg), Gd(NO₃)₃·6H₂O (45.14 mg), and Dy(NO₃)₃·6H₂O (45.66 mg) using otherwise identical procedures, **1-Tb**, **1-Gd**, and **1-Dy** were obtained respectively. **1-Tb**: Yield: ~24.0 mg (76.6% based on H₄L), Anal. Calc. for C₅₈H₉₈Tb₃N₇O₄₅: C, 33.33; H, 4.73; N, 4.69. Found: C, 33.46; H, 4.59; N, 4.72%. IR (KBr, cm⁻¹): 3418(s), 2932(m), 2492(w), 2322(w), 2025(w), 1547(m), 1389(w), 1323(m), 1280(m), 1252(m), 1179(s), 1100(s), 1062(m), 930(m), 860(m), 783(s), 719(s), 657(s), 529(m). **1-Gd**: Yield: ~25.2 mg (82.1% based on H₄L), Anal. Calc. for C₅₈H₉₄Gd₃N₇O₄₃: C, 34.00; H, 4.62; N, 4.79. Found: C, 33.43; H, 4.76; N, 4.83%. IR (KBr, cm⁻¹): 3404(s), 2933(m), 2493(w), 2318(w), 2026(w), 1662(m), 1435(w), 1325(m), 1280(m), 1252(m), 1179(s), 1102(s), 1062(m), 930(m), 861(m), 783(s), 720(s), 657(s), 529(m). **1-Dy**: Yield: ~22.9 mg (73.9% based on H₄L), Anal. Calc. for C₅₈H₉₄Dy₃N₇O₄₃: C, 33.74; H, 4.59; N, 4.75. Found: C, 33.57; H, 4.36; N, 4.69%. IR (KBr, cm⁻¹): 3421(s), 2932(m), 2479(w), 2321(w), 2026(w), 1660(m), 1436(w), 1322(m), 1279(m), 1253(m), 1180(s), 1104(s), 1060(m), 930(m), 862(m), 781(s), 720(s), 657(s), 543(m).

Crystallography. The diffraction data were collected at 295(2) and 100(2) K for **1-Eu** and **1-Gd**,

respectively, with a Bruker-AXS SMART CCD area detector diffractometer using ω rotation scans with a scanwidth of 0.3° and Mo $K\alpha$ radiation ($\lambda = 0.71073 \text{ \AA}$). Absorption corrections were carried out utilizing SADABS routine.¹ The structures were solved by direct methods and refined using the *SHELXTL 97* software.² Atoms were located from iterative examination of difference F-maps following least squares refinements of the earlier models. All the atoms except hydrogen atoms, which were fixed at calculated positions and refined by using a riding mode, were refined anisotropically until full convergence was achieved. The large voids in the structure allow for considerable flexing and uncertainty in the positions of the framework atoms and this is evidenced in large atomic displacement parameters for many of the pyridine carbons, nitrogens from ligand. It was necessary to constrain or restrain a number of bond lengths and angles in the structure in order get a stable refinement and chemically reasonable model. All carbon and nitrogen atoms from pyridine were restrained to have similar ADP's as their neighbors with *simu* and *delu* command in the refinement. The large cage of the unit was occupied by extremely electron density, which could be assigned to be $\text{H}_2\text{N}(\text{Me})_2$ counteranions and free solvent molecules. Because these guest solvents in the crystal is highly disordered and impossible to refine using conventional discrete-atom models, the SQUEEZE³ subroutine of the PLATON software suite was applied to remove the scattering from the highly disordered solvent molecules, and sets of solvent-free diffraction intensities were produced.

The structures of **1-Tb** and **1-Dy** were not measured by single crystal X-ray diffraction, however, which are isostructural with **1-Eu** and **1-Gd**, confirmed by the same crystal shapes and very similar power X-ray diffraction patterns in **Fig. S3**.

The final formulas for the complexes were determined by combining single crystal structures, IR, elemental microanalysis and TGA data.

Crystal data for **1-Eu**: $\text{C}_{50}\text{N}_4\text{O}_{23}\text{H}_{36}\text{Eu}_3$, $M = 1516.71$, Cubic *Im-3*, $a = b = c = 37.9826(10) \text{ \AA}$, $V = 54797(2) \text{ \AA}^3$. $Z = 24$, $D_c = 1.103 \text{ g cm}^{-3}$, $\mu = 2.086 \text{ mm}^{-1}$, $R_{\text{int}} = 0.0534$, final $R_1 = 0.1332$, $wR_2 = 0.3266$ for 9417 unique reflections ($I \geq 2\sigma$), $S = 1.036$. Crystal data for **1-Gd**: $\text{C}_{50}\text{N}_4\text{O}_{23}\text{H}_{36}\text{Gd}_3$, $M = 1532.58$, Cubic *Im-3*, $a = b = c = 37.9569(9) \text{ \AA}$, $V = 54686(2) \text{ \AA}^3$. $Z = 24$, $D_c = 1.117 \text{ g cm}^{-3}$, $\mu = 2.209 \text{ mm}^{-1}$, $R_{\text{int}} = 0.0676$, final $R_1 = 0.1306$, $wR_2 = 0.4069$ for 9389 unique reflections ($I \geq 2\sigma$), $S = 1.947$. CCDC-998805 and 998812 contains the crystallographic data of **1-Eu** and **1-Gd** for this paper.

References

- 1) Bruker. *SADABS*, *SMART* and *SAINT*. Bruker AXS Inc., Madison, Wisconsin, USA, 2002.
- 2) G. M. Sheldrick, *SHELXL-97*, program for the refinement of the crystal structures. University of Göttingen, Germany, 1997.
- 3) Spek, A. L. *Acta Crystallogr., Sect. A*, 1990, 46, C34.

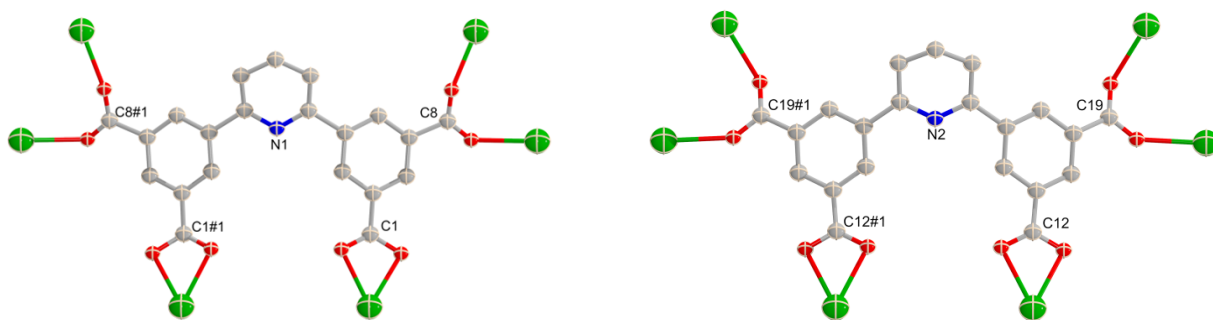


Fig. S1 The bridging fashions of the carboxylate groups of two different L^4 in **1-Eu**. Symmetry codes: #1 x, 2-y, z.

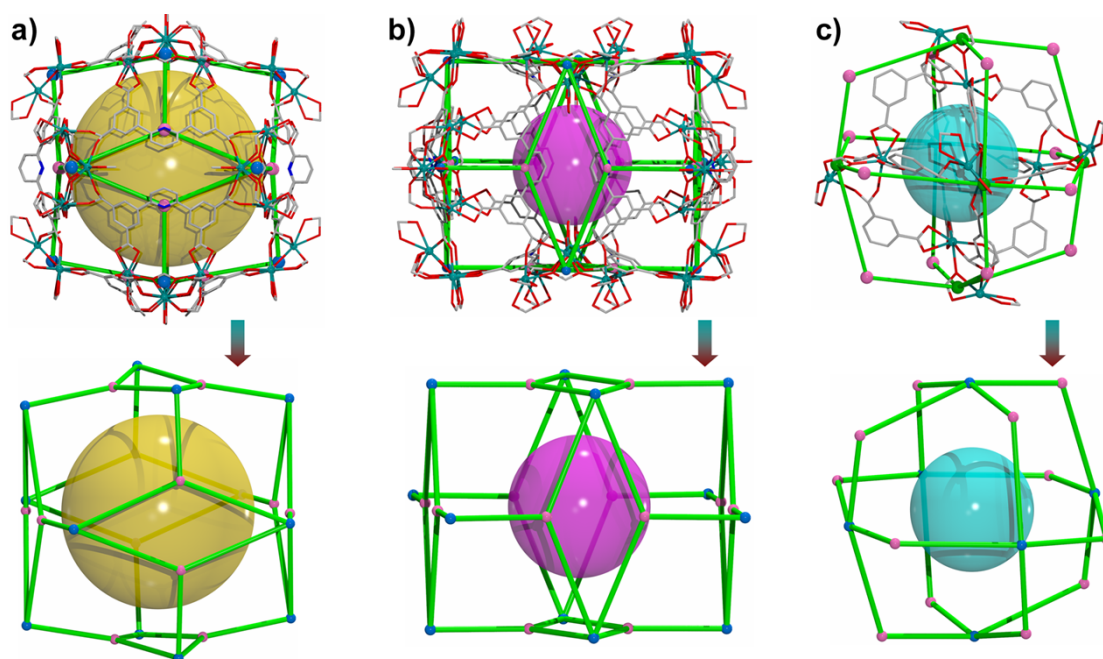


Fig. S2 Three kinds of nanocages in **1-Eu**: a) cage **A**, b) cage **B**, c) cage **C**, and their simplified nets.

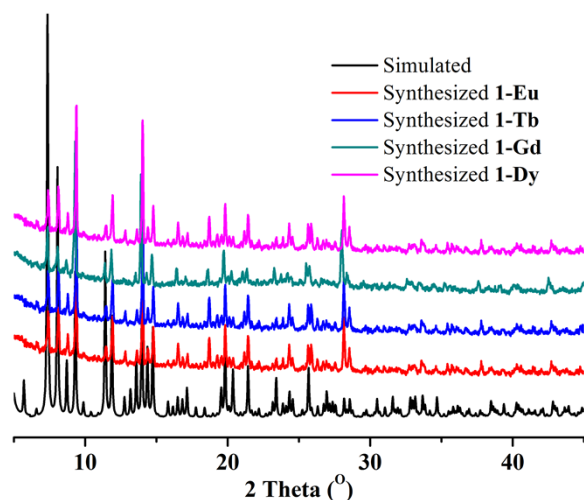


Fig. S3 PXRD patterns of **1-Eu** simulated from the X-ray single-crystal structure and as-synthesized samples of **1-Eu**, **1-Tb**, **1-Gd** and **1-Dy**. The very similar PXRD patterns confirmed the isostructural frameworks of four complexes.

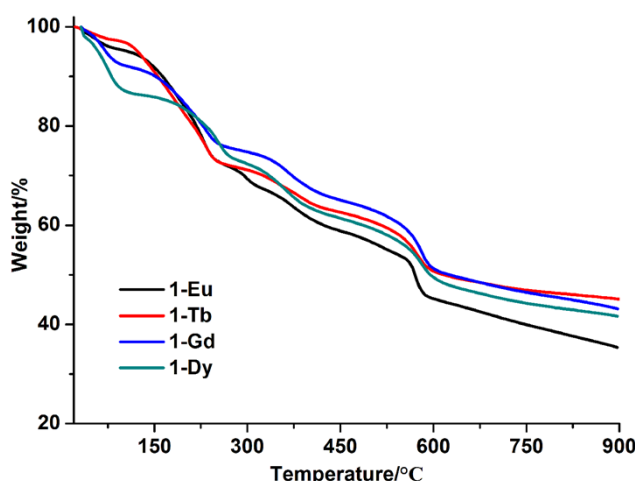


Fig. S4 TGA plots of **1-Ln** under N_2 environment. TGA plots of **1-Ln** reveal similar weight loss processes, which lose all guest solvents below around 235–250 °C. For **1-Eu**, a total weight loss of 24.6% at 32–235 °C, corresponding to the loss of 2DMF and 20 H_2O guest molecules per formula unit (calc. 24.5%). For **1-Tb**, a total weight loss of 24.7% at 32–235 °C, corresponding to the loss of 2DMF and 20 H_2O guest molecules per formula unit (calc. 24.2%). For **1-Gd**, a total weight loss of 23.1% at 32–246 °C, corresponding to the loss of 2DMF and 18 H_2O guest molecules per formula unit (calc. 22.9%). For **1-Dy**, a total weight loss of 22.7% at 32–250 °C, corresponding to the loss of 2DMF and 18 H_2O guest molecules per formula unit (calc. 22.8%), the further releases of aqua and DMF ligands. Above 320–390 °C, these frameworks begin to collapse with the loss of other organic molecules.

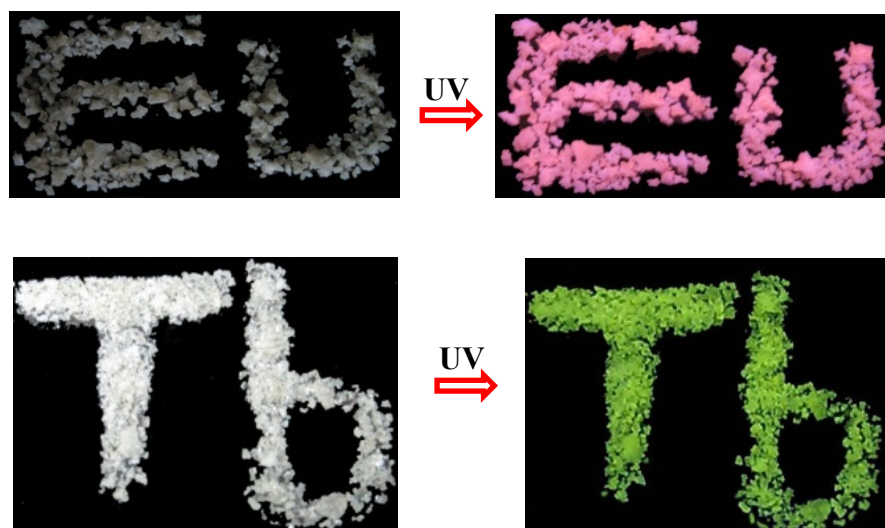


Fig. S5 The snapshots of **1-Eu** and **1-Tb** under UV light (365 nm).

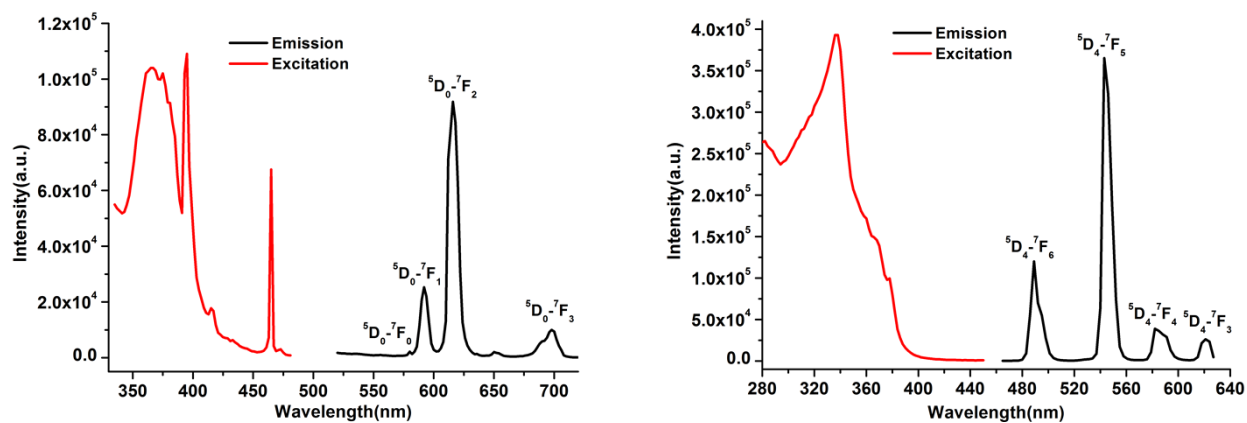


Fig. S6 The excitation and emission spectra of **1-Eu** (left) and **1-Tb** (right).

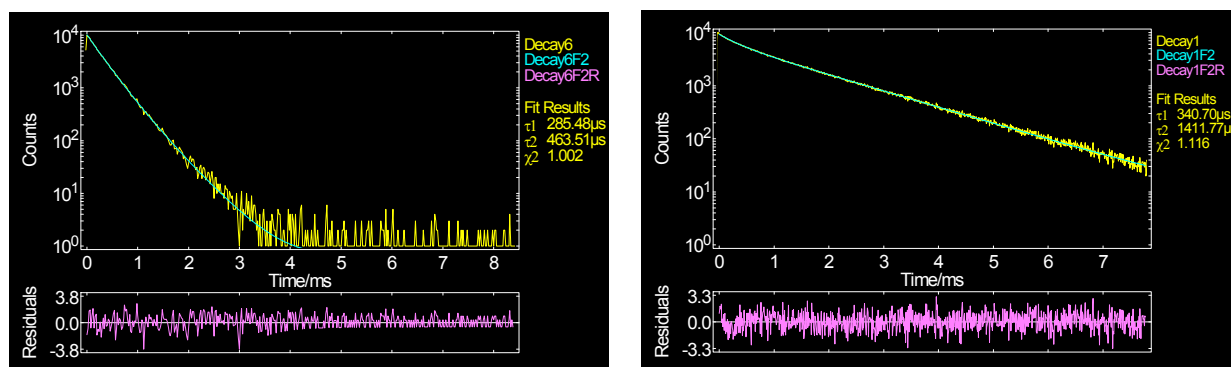


Fig. S7 The luminescence decays of **1-Eu** (left) and **1-Tb** (right) monitored at corresponding excitation/emission maxima.

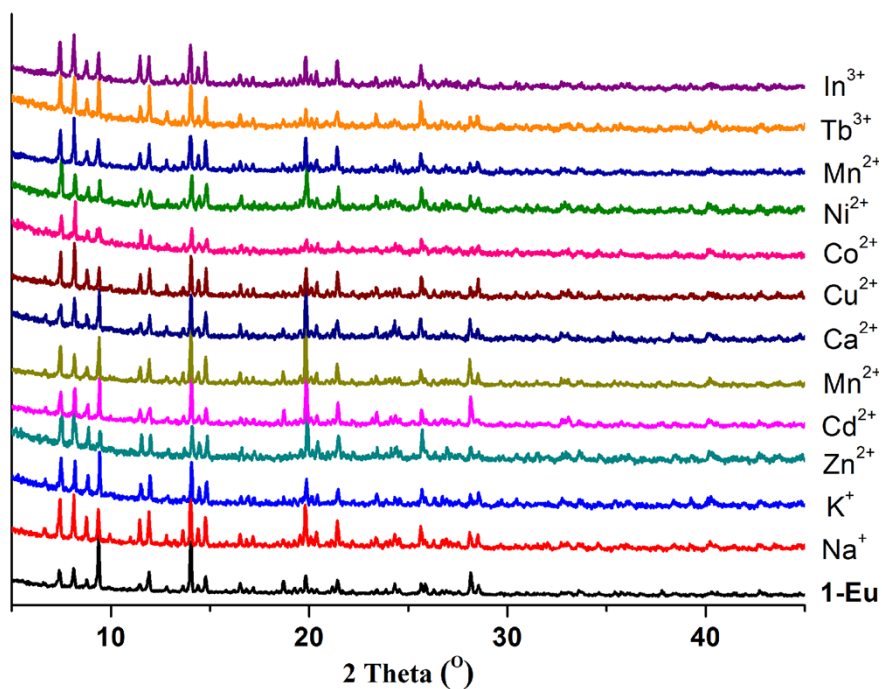


Fig. S8 The PXRD patterns of **1-Eu** treated by different $M(\text{NO}_3)_x$ ($M = \text{Na}^+, \text{K}^+, \text{Mg}^{2+}, \text{Ca}^{2+}, \text{Zn}^{2+}, \text{Cd}^{2+}, \text{Mn}^{2+}, \text{Co}^{2+}, \text{Cu}^{2+}, \text{Ni}^{2+}, \text{Tb}^{3+}$ and In^{3+}) DMF solutions. Based on the XRD patterns, **1-Eu** retains its framework after immersed in DMF solution containing different metal ions.

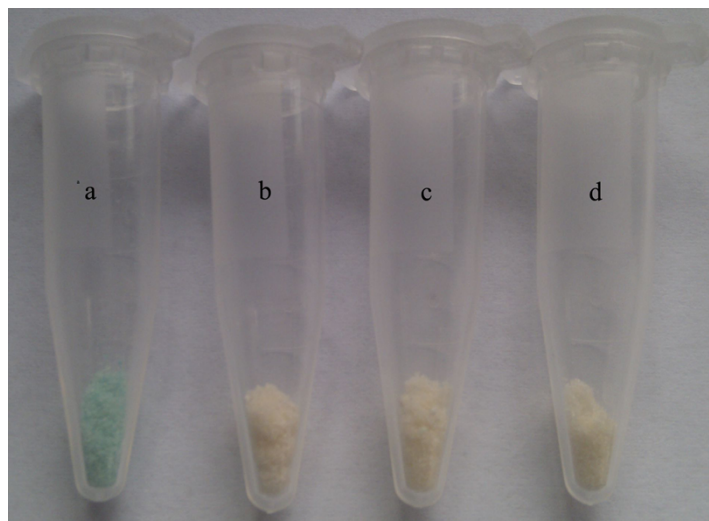


Fig. S9 Photographs of crystals of **1-Eu** soaked in DMF solution containing $M(\text{NO}_3)_2$ with 10^{-1} M, a) Cu^{2+} , b) Co^{2+} , c) Ni^{2+} , d) Mn^{2+} for 24 h, indicating selective color changes for Cu^{2+} .

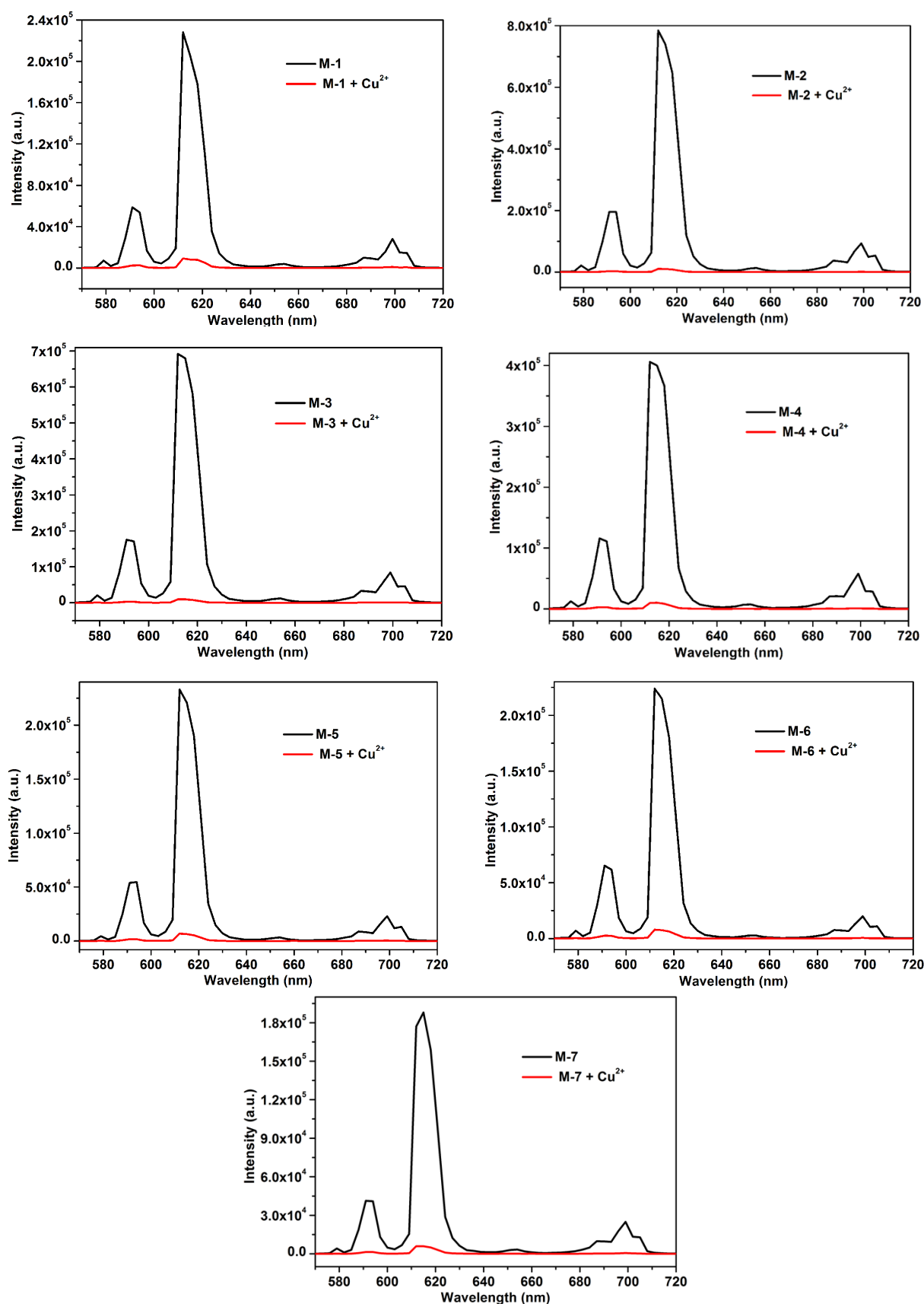


Fig. S10 The luminescence spectra of **1-Eu** in DMF with different mixed metal ions (10^{-1} M) in the absence (black) and presence (red) of Cu^{2+} ion (10^{-2} M). M-1: **1-Eu**, M-2: **1-Eu** + $\text{Na}^+/\text{Mg}^{2+}/\text{Ca}^{2+}$, M3: **1-Eu** + $\text{Mg}^{2+}/\text{Ca}^{2+}$, M4: **1-Eu** + $\text{Zn}^{2+}/\text{Cd}^{2+}$, M5: **1-Eu** + $\text{Co}^{2+}/\text{Ni}^{2+}$, M6: **1-Eu** + $\text{Zn}^{2+}/\text{Cd}^{2+}/\text{Ni}^{2+}$, M-7: **1-Eu** + $\text{Zn}^{2+}/\text{Cd}^{2+}/\text{Co}^{2+}$.

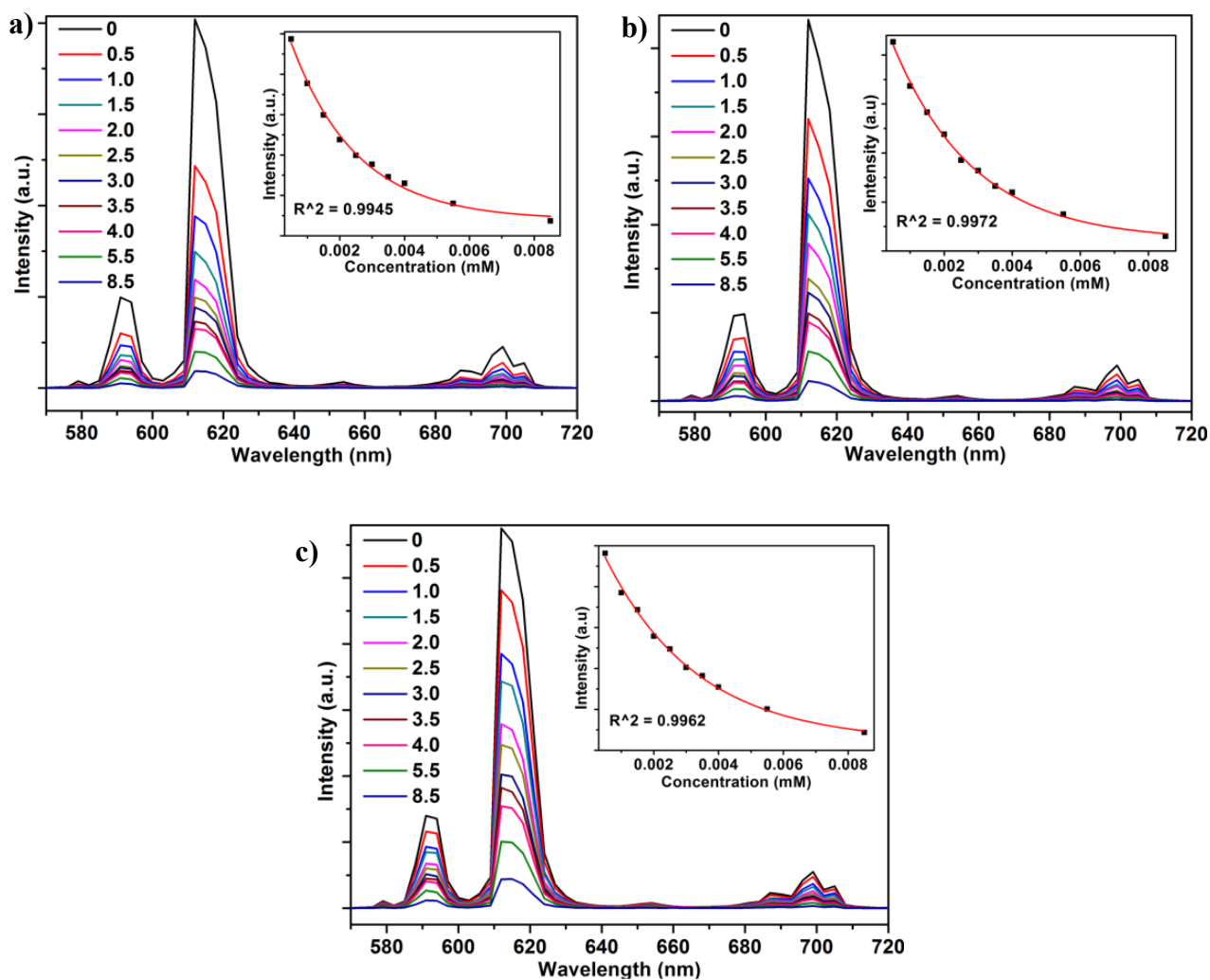


Fig. S11 The luminescence spectra of **1-Eu** in mixed metal ions (10^{-1} M) a) $\text{Na}^+/\text{Mg}^{2+}/\text{Ca}^{2+}$, b) $\text{Co}^{2+}/\text{Ni}^{2+}$ and c) $\text{Zn}^{2+}/\text{Co}^{2+}/\text{Ni}^{2+}$ in the presence of different amounts of Cu^{2+} (mM). Inset: the fitted plot of intensity versus Cu^{2+} ion concentration.

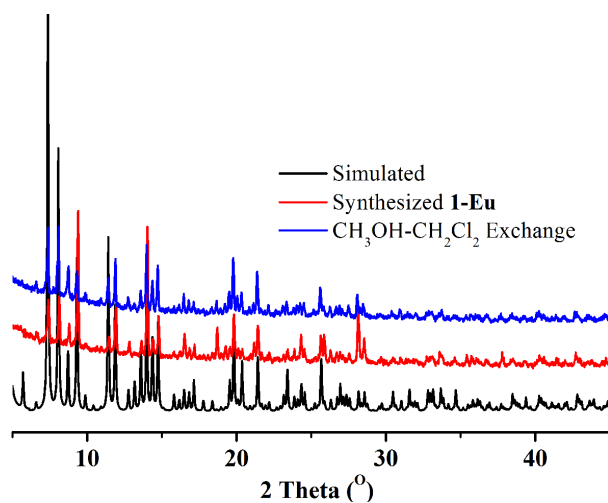


Fig. S12 PXRD patterns of **1-Eu** simulated from the X-ray single-crystal structure, as-synthesized and $\text{CH}_3\text{OH}-\text{CH}_2\text{Cl}_2$ exchanged samples.

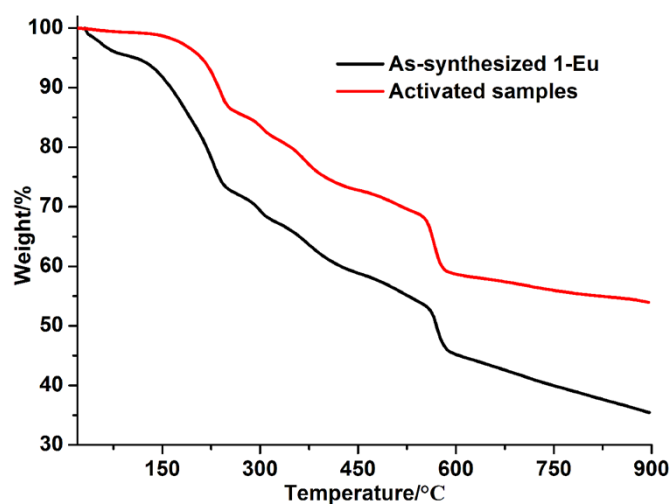


Fig. S13 TGA plots of the as-synthesized and activated samples of **1-Eu**.

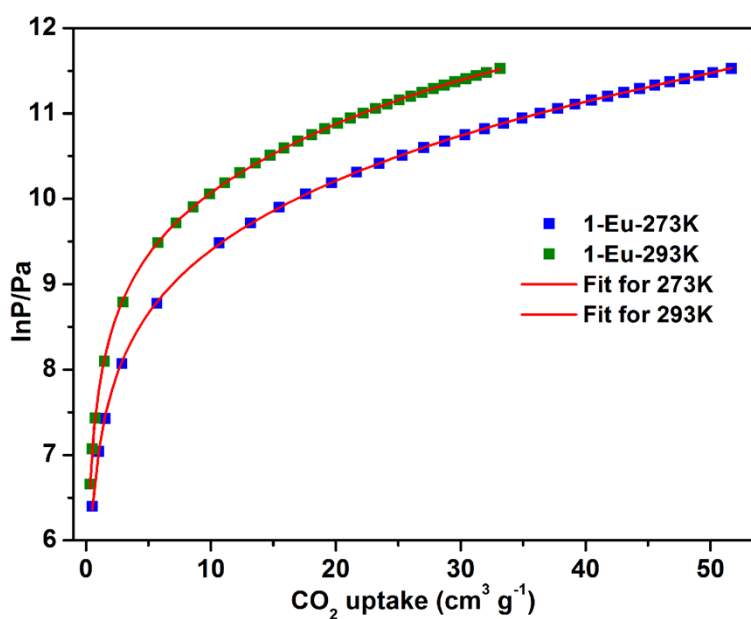


Fig. S14 Virial analysis of the CO₂ sorption data for **1-Eu**. ($a_0 = -2846.45706 \pm 39.61158$, $a_1 = 25.93085 \pm 11.35286$, $a_2 = -1.20980 \pm 0.78418$, $a_3 = 0.01919 \pm 0.01509$, $a_4 = 0.00004 \pm 0.00001$, $b_0 = 17.45728 \pm 0.13924$, $b_1 = -0.09435 \pm 0.03964$, $b_2 = 0.00517 \pm 0.00272$, $b_3 = -0.00008 \pm 0.00005$, $\chi^2 = 0.00013$, $R^2 = 0.99992$.)

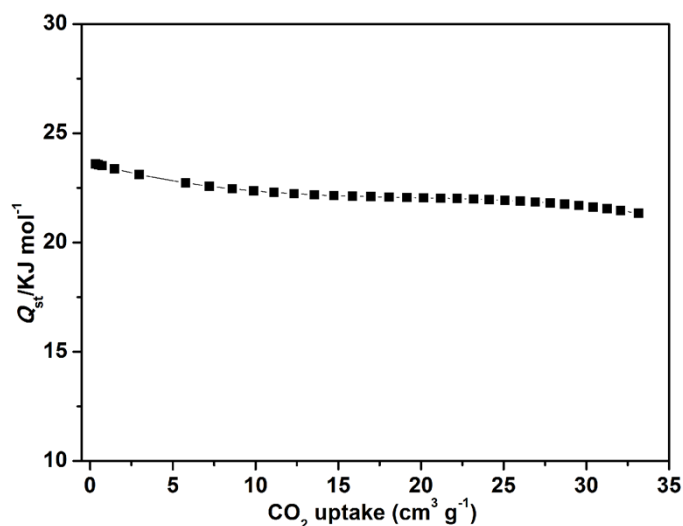


Fig. S15 Heat of CO₂ adsorption for **1-Eu** estimated by the virial equation.

Table S1. Quenching effect coefficients (K_{sv}) of different metal ions on the luminescence intensity of metal-ion-incorporated **1-Eu**, calculated by Stern–Volmer equation: $I_0/I = 1+K_{sv}[M]$, in which the values I_0 and I are the luminescent intensity of metal-ion-free **1-Eu** in DMF and metal-ion-incorporated **1-Eu** in DMF, respectively, $[M]$ is the molar concentration of metal ion, and K_{sv} is the quenching effect coefficient of metal ion (see reference *Angew. Chem. Int. Ed.*, 2009, **48**, 500). The results were shown below.

Metal ion	K_{sv} [M^{-1}]
Ca ²⁺	-64
Tb ³⁺	-63
Mg ²⁺	-57
Zn ²⁺	-54
In ³⁺	-49
Cd ²⁺	-40
Mn ²⁺	-33
Ni ²⁺	-30
Co ²⁺	-19
Na ⁺	-9
K ⁺	1
Cu ²⁺	2.35×10^3

Table S2. Quenching effect coefficients (K_{sv}) of Cu^{2+} ion (10^{-2} M) in **1-Eu** and mixed metal ions (10^{-1} M) systems.

Mixed metal ions	K_{sv} [M^{-1}]
$\text{Na}^+/\text{Mg}^{2+}/\text{Ca}^{2+}$	7.31×10^3
$\text{Mg}^{2+}/\text{Ca}^{2+}$	7.12×10^3
$\text{Zn}^{2+}/\text{Cd}^{2+}$	4.17×10^3
$\text{Co}^{2+}/\text{Ni}^{2+}$	3.32×10^3
$\text{Zn}^{2+}/\text{Cd}^{2+}/\text{Ni}^{2+}$	2.75×10^3
$\text{Zn}^{2+}/\text{Cd}^{2+}/\text{Co}^{2+}$	2.89×10^3